



Cite this: *Green Chem.*, 2017, **19**, 2096

Received 20th February 2017,
Accepted 3rd April 2017

DOI: 10.1039/c7gc00539c

rsc.li/greenchem

Visible-light-driven photooxidation of alcohols using surface-doped graphitic carbon nitride†

Wuyuan Zhang,^a Anna Bariotaki,^b Ioulia Smonou^b and Frank Hollmann^a

Carbon-nanodot-doped g-C₃N₄ is used as a photocatalyst to promote the aerobic oxidation of alcohols and oxyfunctionalisation of activated hydrocarbons. A critical E-factor analysis of the current reaction system reveals its limitations *en route* to environmentally acceptable oxidation procedures.

In recent years, graphitic carbon nitride (g-C₃N₄) has received substantial interest as a photocatalyst for metal-free, visible-light promoted reactions.¹ It exhibits a graphite-like, layered structure wherein tris-triazine units are connected through C–N-bonds forming a two-dimensional layer. g-C₃N₄ can be synthesized *via* various methods such as pyrolysis of urea or other nitrogen-rich precursors or layer exfoliation of bulk materials.²

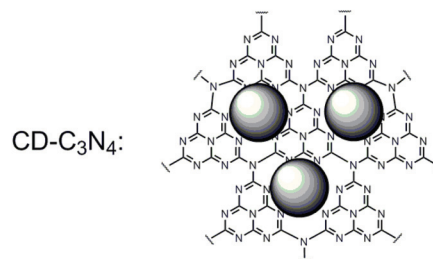
Pure g-C₃N₄, however, is a rather poor photocatalyst, mainly due to the fast recombination of photoexcited, charge-separated states. Therefore, one focus of research lies in the improvement of its photocatalytic properties by modulating the potential of g-C₃N₄'s conducting- and valence bands.¹ Particularly doping of g-C₃N₄ with other elements such as Y,³ Fe,⁴ Pt,⁵ Au/Pd,^{6,7} K, Ag,^{8,9} C¹⁰ or carbon-nanodots¹¹ and many more has proven to be an efficient handle to modulate its properties. Also, doping with carbon-nanodots appears promising to increase the quantum efficiency of photocatalytic processes.

Interestingly, g-C₃N₄ is mostly considered as a photocatalyst for (sun)-light driven water splitting, remediation of organic pollutants and catalytic CO₂ reduction.¹ Applications for preparative organic synthesis are comparably few. For example, Goettmann *et al.* reported g-C₃N₄ catalysed Friedel–Crafts acylation.¹² More recently, photocatalytic acetalisation of aldehydes and ketones,¹³ and hydrazine-driven reductions of alkenes and alkynes were reported using g-C₃N₄.^{14,15} Selective

oxidations especially of benzylic C–H-bonds have been reported using mesoporous g-C₃N₄ together with N–OH-cocatalysts,^{16–19} or using transition metal doped g-C₃N₄.^{14,20–22} Also the oxidative coupling of amines has been reported.²³

However, to the best of our knowledge, carbon-nanodot doped g-C₃N₄ has so far not been evaluated as a catalyst for photocatalytic oxidation reactions. Therefore, we set out to evaluate carbon-nanodot-doped g-C₃N₄ (CD-C₃N₄) as a visible-light-driven photocatalyst for the aerobic oxidation of alcohols (Scheme 1).

For the synthesis of g-C₃N₄ we followed the procedure by Tang and coworkers²⁴ due to the more porous structure of the material and the resulting higher activity (due to the increased surface area). In short, calcination of urea at 600 °C for 4 h gave the desired mesoporous g-C₃N₄ as confirmed by TEM imaging and X-ray diffraction (Fig. S1 and S2†). Next, carbon nanodots were synthesized *via* thermal decomposition of sucrose.²⁵ The latter were deposited on the g-C₃N₄ surface *via* thermal treatment of both materials.¹¹ The XRD pattern of the such-obtained composite material did not change significantly compared to the starting material (g-C₃N₄) most probably due to the amorphous character of the carbon nanodots adsorbed.



Scheme 1 Photocatalytic aerobic oxidation using carbon nanodot-doped g-C₃N₄ (CD-C₃N₄) as a photocatalyst.

^aDepartment of Biotechnology, Delft University of Technology, Van der Maasweg 9, 2629HZ Delft, The Netherlands. E-mail: W.Zhang-1@tudelft.nl, F.Hollmann@tudelft.nl

^bDepartment of Chemistry, University of Crete, Heraklion-Voutes 71003, Crete, Greece

† Electronic supplementary information (ESI) available: Details of the experimental procedures and additional analytic material. See DOI: 10.1039/c7gc00539c



The UV/Vis spectrum showed the characteristic increase in absorption at wavelengths below 600 nm (Fig. S3†), and the BET measurement revealed a surface area of $105 \text{ m}^2 \text{ g}^{-1}$ (Fig. S8†).

Having both catalysts at hand, we next compared their catalytic activity in the oxidation of benzyl alcohol to benzaldehyde as a model reaction (Fig. 1). Due to the volatility of benzaldehyde and the poor water solubility of the benzyl alcohol starting material we used a two-liquid phase approach employing benzyl alcohol as the second organic phase (phase ratio 3 : 7 organic : aqueous).

As shown in Fig. 1, CD- C_3N_4 excelled over g- C_3N_4 both in terms of activity and robustness. Not only was the initial product formation rate roughly two times higher but also the long term-stability of the reaction: the reaction rate with g- C_3N_4 levelled off significantly after several hours whereas with CD- C_3N_4 linear product accumulation was observed for at least 48 h. Overall, with CD- C_3N_4 more than 500 mM of product accumulated corresponding to a product to catalyst ratio of more than 4 : 1 (g g^{-1}), under the non-optimized conditions.

It is worth mentioning here, that in the absence of either the photocatalyst or a light source, no noticeable conversion of the starting material was observed. Also, hydrogen peroxide as a by-product was observable in trace amounts only throughout the experiments. This observation is in line with previous findings that CD- C_3N_4 is also an efficient H_2O_2 decomposition catalyst.¹¹

The rate of the oxidation reaction exhibited a saturation-type dependency on both the catalyst concentration (Fig. 2) and the intensity of the light source applied (Fig. 3).

In the case of increasing catalyst concentrations, we suspect the decreasing transparency of the reaction mixture to account

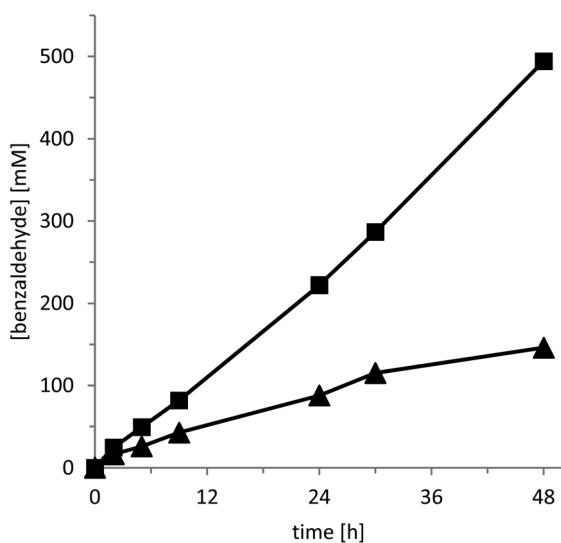


Fig. 1 Photocatalytic oxidation of benzyl alcohol to benzaldehyde using g- C_3N_4 (\blacktriangle) and CD- C_3N_4 (\blacksquare) as photocatalysts. Conditions: 5 g L^{-1} of photocatalyst, two phase reaction: $700 \mu\text{L}$ of water + $300 \mu\text{L}$ of benzyl alcohol, $30 \text{ }^\circ\text{C}$ and oxygen atmosphere under visible light illumination using setup 1 ($\lambda > 400 \text{ nm}$).

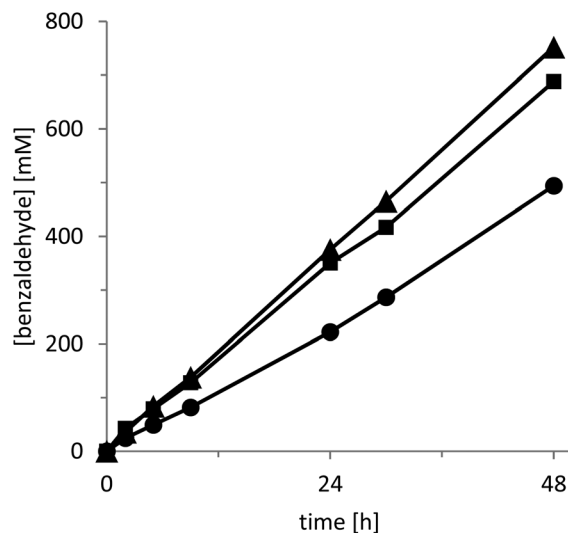


Fig. 2 Influence of the catalyst loading on the rate of the photocatalytic oxidation of benzyl alcohol. [CD- C_3N_4] = 5 (\bullet), 10 (\blacksquare), 25 (\blacktriangle) g L^{-1} . Conditions: Two phase reaction with $700 \mu\text{L}$ of water + $300 \mu\text{L}$ of benzyl alcohol, $30 \text{ }^\circ\text{C}$ and oxygen atmosphere under visible light illumination using setup 1 ($\lambda > 400 \text{ nm}$).

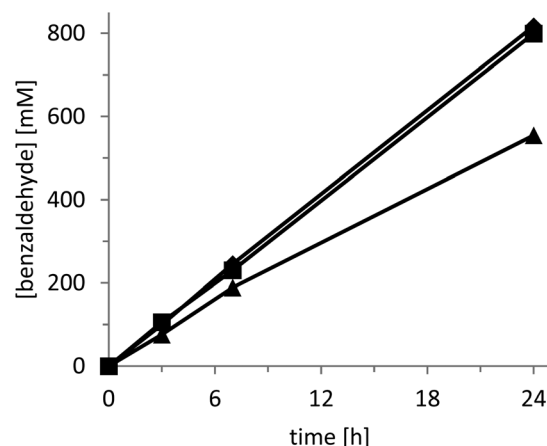


Fig. 3 Influence of the light intensity on the rate of the photocatalytic oxidation of benzyl alcohol. Light intensity of 79 (\blacktriangle), 197 (\blacksquare), 341 (\blacklozenge) W cm^{-2} . Conditions: 5 g L^{-1} of photocatalyst, two phase reaction with $700 \mu\text{L}$ of water + $300 \mu\text{L}$ of benzyl alcohol, $30 \text{ }^\circ\text{C}$ and oxygen atmosphere under visible light illumination using setup 2 ($\lambda > 400 \text{ nm}$).

for this observation. The converging reaction rate at increasing light intensities may well be attributed to oxygen diffusion becoming overall rate-limiting. It should be mentioned here that for the latter experiments we utilised a specialized light-setup to control the light intensity (setup 2, Fig. S5†). Despite the much higher product formation rate attainable with this system (Fig. 3) we decided to perform the following experiment using a cheap white-light bulb in order to enable simple reproduction by others (setup 1, Fig. S4†). Nevertheless, the productivities shown in Fig. 3 (using a simple light source) of more than $0.2 \text{ g}_{\text{product}} \text{ g}^{-1}_{\text{catalyst}} \text{ h}^{-1}$ demonstrate the preparative potential of the photochemical alcohol oxidation system.



We investigated the recyclability of CD-C₃N₄ by performing benzyl alcohol oxidation reactions followed by filtration, washing and re-loading with reaction medium (Fig. S6†). As a result CD-C₃N₄ could be recycled at least 5 times. From linear regression of the initial rates, a catalyst deactivation of less than 4% per cycle was estimated.

Encouraged by these results we further explored the product scope of the reaction system (Table 1).

Especially allylic alcohols were converted at excellent rates and selectivities while benzylic alcohols were converted somewhat slower and non-activated alcohols such as cyclohexanol were rather sluggish substrates. This is roughly in-line with the general bond-dissociation energies of the C–H bonds oxidised. However, it also should be taken into account that the reactions reported in Table 1 have been obtained from two-liquid phase systems and that, depending on the partitioning coefficient of

the starting material, the aqueous concentrations may vary very significantly thereby influencing the reaction kinetics.

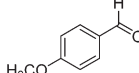
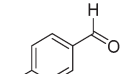
The preparative applicability of the proposed photocatalytic oxidation was exemplarily demonstrated in the oxidation of carveol to carvone. Performing this reaction on a 6.8 mmol-scale (1.03 g) gave more than 95% conversion into the desired product (GC yield) and 0.773 g of isolated carvone (74.8% isolated yield) under non-optimised reaction- and DSP conditions.

An E-factor analysis²⁶ of this reaction revealed the current limitations of this reaction setup from an environmental point-of-view (Table 2). The ‘classical’ E-factor (including the weighable compounds only) of the overall reaction is rather moderate (144) with solvents (used both for the reaction and for the extraction of the product) contributing over 95% to the total E-factor. Obviously, dichloromethane used in this reaction is not acceptable and will be substituted by more acceptable solvents in future studies.²⁷ Also decreasing the contribution of water (*e.g.* by further increasing the concentration of the starting material) will be highly desirable. In fact, preliminary experiments using neat reagents (*i.e.* CD-C₃N₄ suspended in pure benzyl alcohol or cyclohexanol) showed an even faster product accumulation than in the biphasic system (Fig. S7†). Probably this is also to be attributed to a higher O₂ solubility in these media than in aqueous systems. Another advantage of using neat reagents is that extraction can be omitted as physical methods to separate the product (*e.g.* distillation) are sufficient.

However, the ‘hidden’ E-factor contributors demand more attention *en route* to an environmentally acceptable reaction system. Using setup 2 enabled us to quantify the power input (197 W for 90 h) and energy used for the illumination reaction (17.7 kWh). According to the European Energy Agency this corresponds to CO₂ emission of approximately 9.9 kg CO₂²⁸ and an E-factor contribution of 12.800 obviously ‘outshining’ the values discussed above. Of course the current setup has not been optimised for efficient utilisation of light and further geometric optimisation together with the increase of the reagent payload will certainly reduce this number to acceptable values. Also, provided the aspirational trend towards renewable energies continues, less CO₂ emissions and thereby a reduced ‘CO₂’-E-factor may be assumed. Furthermore, using sunlight will almost entirely eliminate this contribution.

Also, it should not be forgotten that the preparation of the photocatalyst (though exhibiting very low classical E-factors) is based on high-temperature calcination processes.

Table 1 Examples of CD-C₃N₄-catalyzed, photocatalytic alcohol oxidations

Product	Product ^a [mM]	Rate [g g ⁻¹ h ⁻¹]
	223	0.059
	60.1	0.020
	73.0	0.023
	40.2	0.012
	12.7/1.9 ^a	0.003/0.001 ^a
	228.1/41 ^a	0.055/0.023 ^a
	701.2	0.193
	108.4	0.040
	247.3	0.093
	252.4	0.087

Reaction conditions: 5 g L⁻¹ of photocatalyst, two phase reaction with 700 μL of water + 300 μL of alcohol, 30 °C and oxygen atmosphere under visible light illumination using setup 1 (λ > 400 nm) for 24 h. ^a Product concentration in the aqueous phase.

Table 2 Estimation of the waste generated in the photobiocatalytic oxidation of carveol to carvone

Contributor	E-factor contribution [kg kg ⁻¹]
Reaction	
Water	38.8
CD-C ₃ N ₄	0.26
CO ₂ from a light source	12.800
DSP	
CH ₂ Cl ₂	102.8
MgSO ₄	1.9

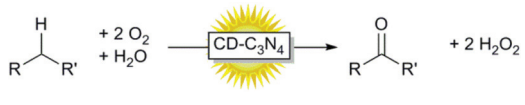


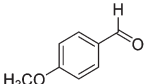
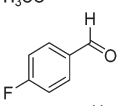
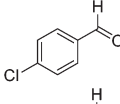
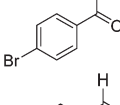
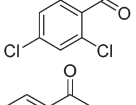
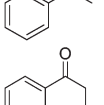
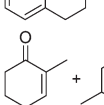
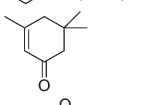
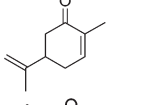
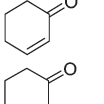
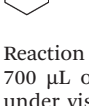
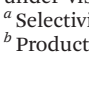
Overall, despite the potential of photochemical, aerobic oxidation we prefer to refrain from calling the current procedure green or environmentally benign.

Finally, we evaluated oxidation/oxyfunctionalisation of non-functionalized C–H bonds (Table 3). In general, the same trend in the reaction rate was observed here as well whereas

the reaction rates were significantly lower than observed for the corresponding alcohols. This is in line with the higher C–H-bond dissociation energy of these non-functionalized C–H bonds. Furthermore, accumulation of the intermediate alcohol product did not occur (generally the alcohol product accounted for less than 25% of the final product) indicating that the initial C–H-bond oxidation is overall rate-limiting.

Table 3 Examples of CD-C₃N₄-catalyzed, photocatalytic oxyfunctionalisations



Product	Product [mM]	Selectivity ^a (%)	Rate [g g ⁻¹ h ⁻¹]
	16.3	77	0.004
	19.0	83.3	0.0065
	3.0	86.2	0.001
	12.6	—	0.0044
	3.9	—	0.002
	4.1	—	0.0018
	7.6	76.9	10.0023
	18.1	87.4	0.0067
	30.3 + 37.7	—	0.008 + 0.010
	28.14	—	0.011
	21.25	—	0.008
	10.3/9.1 ^b	—	0.002/0.005 ^b
	3.0	—	0.0007

Reaction conditions: 5 g L⁻¹ of photocatalyst, two phase reaction with 700 μL of water + 300 μL of alkane, 30 °C and oxygen atmosphere under visible light illumination using setup 2 (λ > 400 nm) for 24 h.

^a Selectivity = [aldehyde/ketone]/([alcohol] + [aldehyde/ketone])%.
^b Product concentration in the aqueous phase.

Conclusions

With the current contribution we demonstrate that simple metal-free CD-C₃N₄ is a very suitable and recyclable photocatalyst for the oxidation of primary and secondary alcohols to the corresponding aldehydes and ketones. Furthermore, also extension of this concept to the corresponding alkanes appears feasible, albeit at reduced efficiencies.

Ongoing mechanistic studies will reveal a more detailed understanding of the reaction and put the basis for optimised catalysts and reaction setups *en route* to truly practical catalysts.

The critical E-factor analysis of the current reaction setup will guide our further studies *en route* to truly environmentally acceptable oxidation processes.

Acknowledgements

Financial support by the European Research Council (ERC Consolidator Grant No. 648026) is gratefully acknowledged. The authors thank Ben Norder (Delft University of Technology) for XRD and Dr Wiel H. Evers (Delft University of Technology) for TEM measurements.

Notes and references

- W.-J. Ong, L.-L. Tan, Y. H. Ng, S.-T. Yong and S.-P. Chai, *Chem. Rev.*, 2016, **116**, 7159–7329.
- J. Liu, H. Wang and M. Antonietti, *Chem. Soc. Rev.*, 2016, **45**, 2308–2326.
- Y. Wang, Y. Li, X. Bai, Q. Cai, C. Liu, Y. Zuo, S. Kang and L. Cui, *Catal. Commun.*, 2016, **84**, 179–182.
- Q. Wang, A. Chen, X. Wang, J. Zhang, J. Yang and X. a. Li, *J. Mol. Catal. A: Chem.*, 2016, **420**, 159–166.
- X. Li, W. Bi, L. Zhang, S. Tao, W. Chu, Q. Zhang, Y. Luo, C. Wu and Y. Xie, *Adv. Mater.*, 2016, **28**, 2427–2431.
- C. Han, L. Wu, L. Ge, Y. Li and Z. Zhao, *Carbon*, 2015, **92**, 31–40.
- T. Xiong, W. Cen, Y. Zhang and F. Dong, *ACS Catal.*, 2016, **6**, 2462–2472.
- Y. Fu, T. Huang, L. Zhang, J. Zhu and X. Wang, *Nanoscale*, 2015, **7**, 13723–13733.
- R. Kuriki, H. Matsunaga, T. Nakashima, K. Wada, A. Yamakata, O. Ishitani and K. Maeda, *J. Am. Chem. Soc.*, 2016, **138**, 5159–5170.



- 10 Y. Wang, X. Bai, H. Qin, F. Wang, Y. Li, X. Li, S. Kang, Y. Zuo and L. Cui, *ACS Appl. Mater. Interfaces*, 2016, **8**, 17212–17219.
- 11 J. Liu, Y. Liu, N. Liu, Y. Han, X. Zhang, H. Huang, Y. Lifshitz, S.-T. Lee, J. Zhong and Z. Kang, *Science*, 2015, **347**, 970–974.
- 12 F. Goettmann, A. Fischer, M. Antonietti and A. Thomas, *Angew. Chem., Int. Ed.*, 2006, **45**, 4467–4471.
- 13 M. Abdullah Khan, I. F. Teixeira, M. M. J. Li, Y. Koito and S. C. E. Tsang, *Chem. Commun.*, 2016, **52**, 2772–2775.
- 14 S. Verma, R. B. N. Baig, M. N. Nadagouda and R. S. Varma, *ACS Sustainable Chem. Eng.*, 2016, **4**, 1094–1098.
- 15 R. B. N. Baig, S. Verma, R. S. Varma and M. N. Nadagouda, *ACS Sustainable Chem. Eng.*, 2016, **4**, 1661–1664.
- 16 P. Zhang, J. Deng, J. Mao, H. Li and Y. Wang, *Chin. J. Catal.*, 2015, **36**, 1580–1586.
- 17 F. Z. Su, S. C. Mathew, G. Lipner, X. Z. Fu, M. Antonietti, S. Blechert and X. C. Wang, *J. Am. Chem. Soc.*, 2010, **132**, 16299–16301.
- 18 B. Long, Z. Ding and X. Wang, *ChemSusChem*, 2013, **6**, 2074–2078.
- 19 P. Zhang, Y. Wang, J. Yao, C. Wang, C. Yan, M. Antonietti and H. Li, *Adv. Synth. Catal.*, 2011, **353**, 1447–1451.
- 20 H. Han, G. Ding, T. Wu, D. Yang, T. Jiang and B. Han, *Molecules*, 2015, **20**, 12686.
- 21 Z. Ding, X. Chen, M. Antonietti and X. Wang, *ChemSusChem*, 2011, **4**, 274–281.
- 22 S. Verma, R. B. Nasir Baig, M. N. Nadagouda and R. S. Varma, *ACS Sustainable Chem. Eng.*, 2016, **4**, 2333–2336.
- 23 F. Su, S. C. Mathew, L. Möhlmann, M. Antonietti, X. Wang and S. Blechert, *Angew. Chem., Int. Ed.*, 2011, **50**, 657–660.
- 24 D. J. Martin, K. Qiu, S. A. Shevlin, A. D. Handoko, X. Chen, Z. Guo and J. Tang, *Angew. Chem., Int. Ed.*, 2014, **53**, 9240–9245.
- 25 J. Pan, Y. Sheng, J. Zhang, J. Wei, P. Huang, X. Zhang and B. Feng, *J. Mater. Chem. A*, 2014, **2**, 18082–18086.
- 26 R. A. Sheldon, *Green Chem.*, 2017, **19**, 18–43.
- 27 P. G. Jessop, *Green Chem.*, 2011, **13**, 1391–1398.
- 28 <http://www.eea.europa.eu/> (accessed on 19.02.2017).

